X-ray and Gamma-ray Emission Pulsars and Pulsar Wind Nebulae

K.S. Cheng

Department of Physics

University of Hong Kong

Hong Kong, China

X-ray luminosity (L_x) vs spin-down power (L_{sd})

- Becker and Trumper (1997) used 27 rotation-power pulsars observed by ROSAT (0.1-2.4 KeV) and found **$L_x \sim L_{sd}$**
- Saito (1998) used 16 rotation-power pulsars observed by ASCA (2-10 KeV) and found **$L_x \sim (L_{sd})^{3/2}$**
- Possenti et al. (2002) used ROSAT, ASCA, RXTE, BappoSAX, Chandra, XMM (41 pulsars) to obtain **$L_x \sim (L_{sd})^{1.34}$**

MSPs in the field are included in above three analysis. However

- Grindlay et al.(2002) find MSPs in 47 Tuc satisfy **$L_x \sim (L_{sd})^{1/2}$**

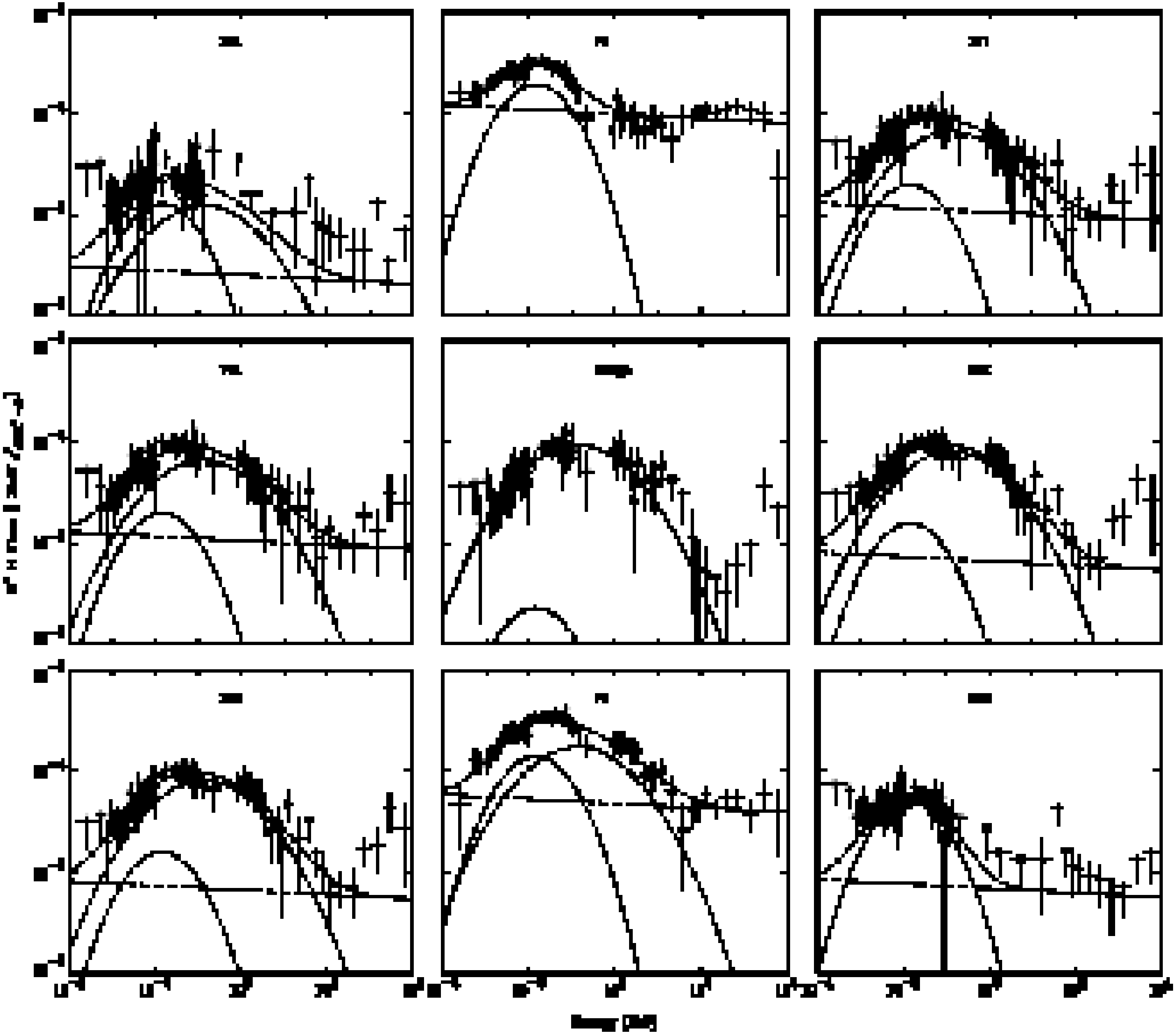

The phase-resolved spectrum of the Crab pulsar

Energy range of the data

100eV-10GeV

(Kuiper etal. 2001)

Radiation Theories of Pulsars and Pulsar Wind Nebulae

- A Self-consistent Outer Gap Model - 3 Dimensional Model
- A Simple Model for Radiation from Pulsar Wind Nebula

Radiation from pulsar magnetospere - 3D pulsar model

Static dipole field
- non-rotating pure dipole

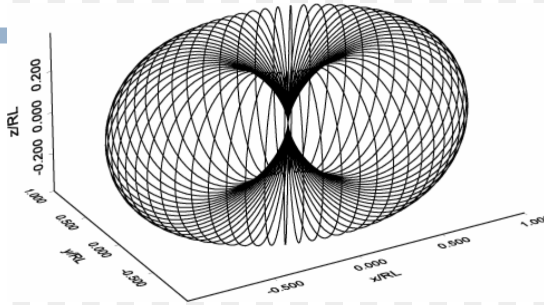

$\alpha = 0$

Retarded magnetic field lines of the rotating and inclined dipole field
- Relativistic effects are taken into account

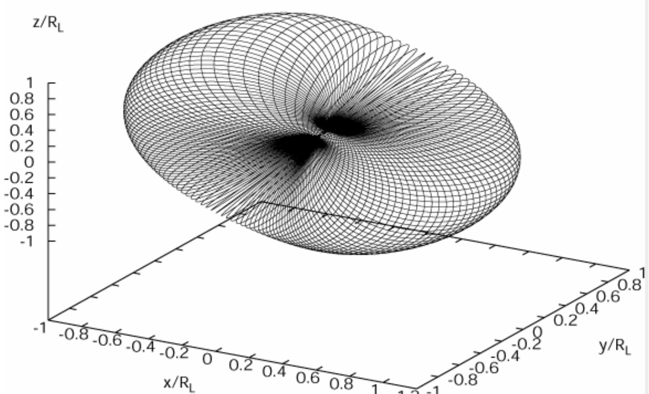

$\alpha = 30^o$

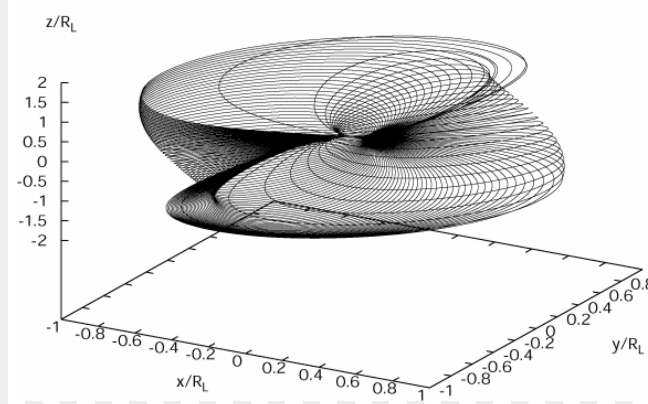

$\alpha = 60^o$

α: magnetic inclination angle

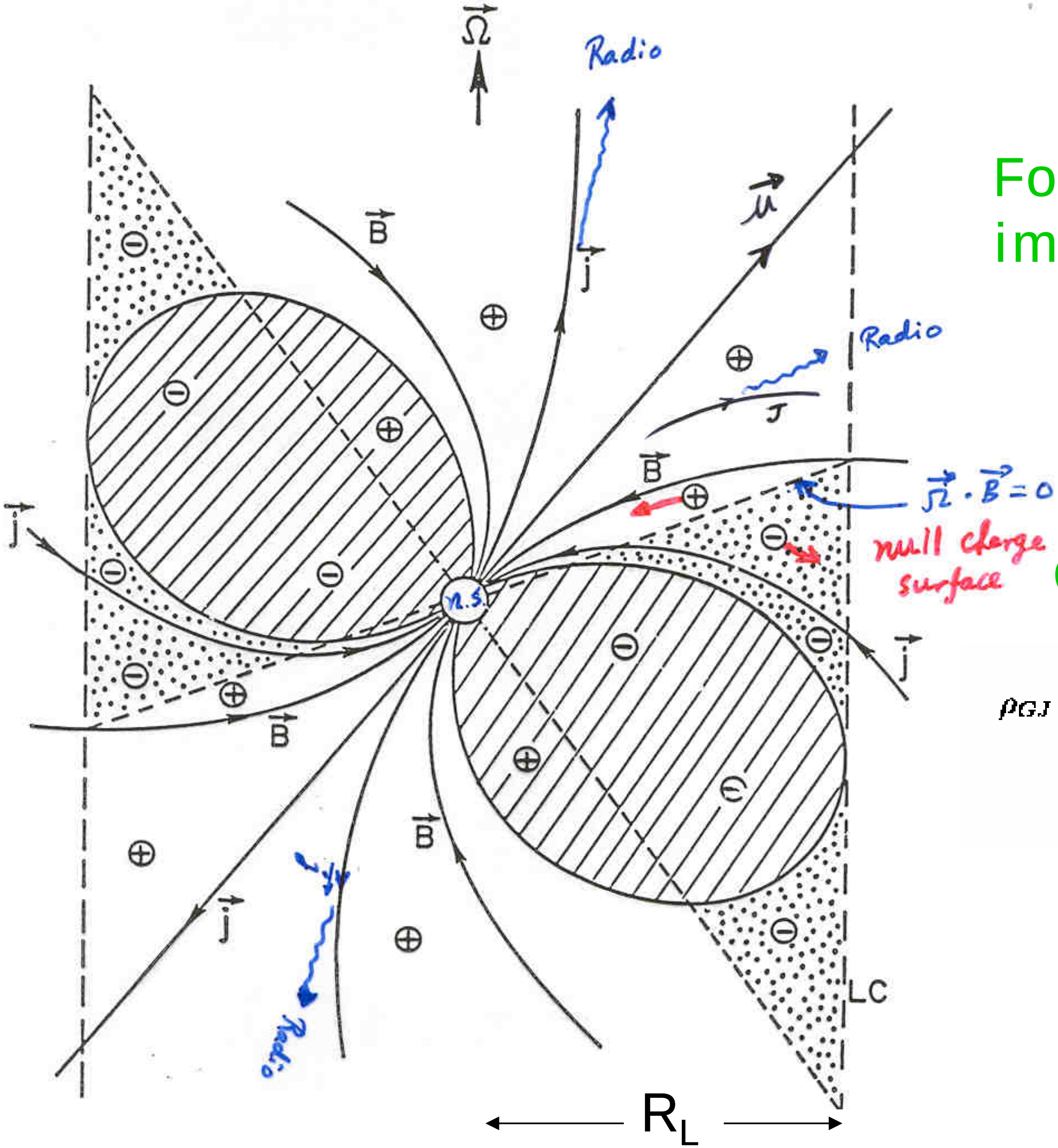

Force free condition implies:

$$\mathbf{E} + \frac{1}{c}(\mathbf{\Omega} \times \mathbf{r}) \times \mathbf{B} = 0$$

Charge distribution:

$$\begin{aligned} \rho_{GJ} &= \frac{1}{4\pi} \nabla \cdot \mathbf{E} \\ &\approx -\frac{\mathbf{\Omega} \cdot \mathbf{B}}{2\pi c} \frac{1}{1 - |\mathbf{\Omega} \times \mathbf{r}/c|^2} \approx -\frac{\mathbf{\Omega} \cdot \mathbf{B}}{2\pi c} \end{aligned}$$

Goldreich-Julian charge density

Pair creation in Outergap where $(\vec{E} \bullet \hat{B}) \neq 0$

The high energy photons emitted by the charged particles in the gap can become pairs by

$$\gamma + x(\text{soft photon}) \rightarrow e^{\pm}$$

These pairs limit the growth of the gap

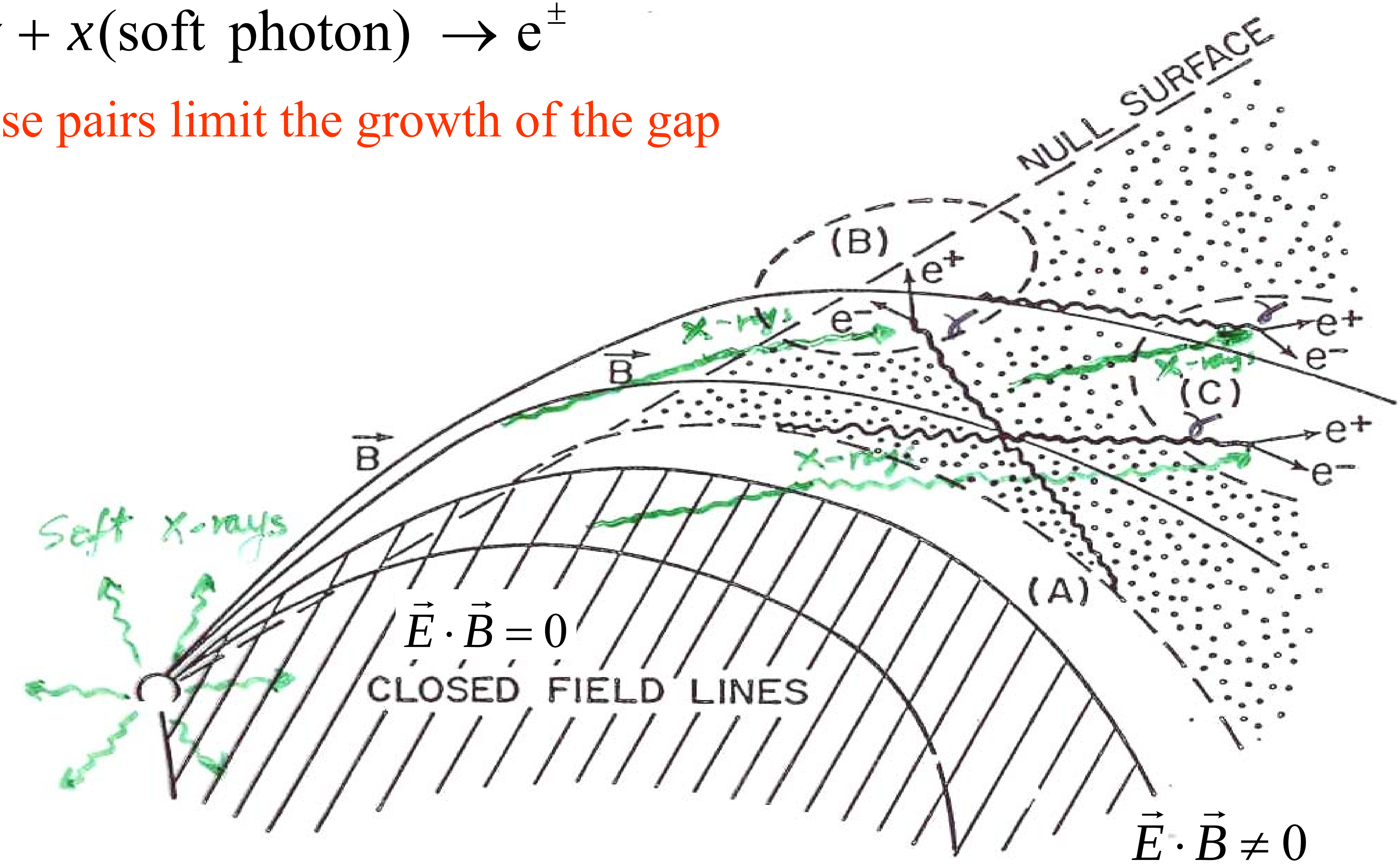

Self-sustained Mechanism - Pair Production and (Thermal and Non-thermal) X-ray emission from near and on NS surface

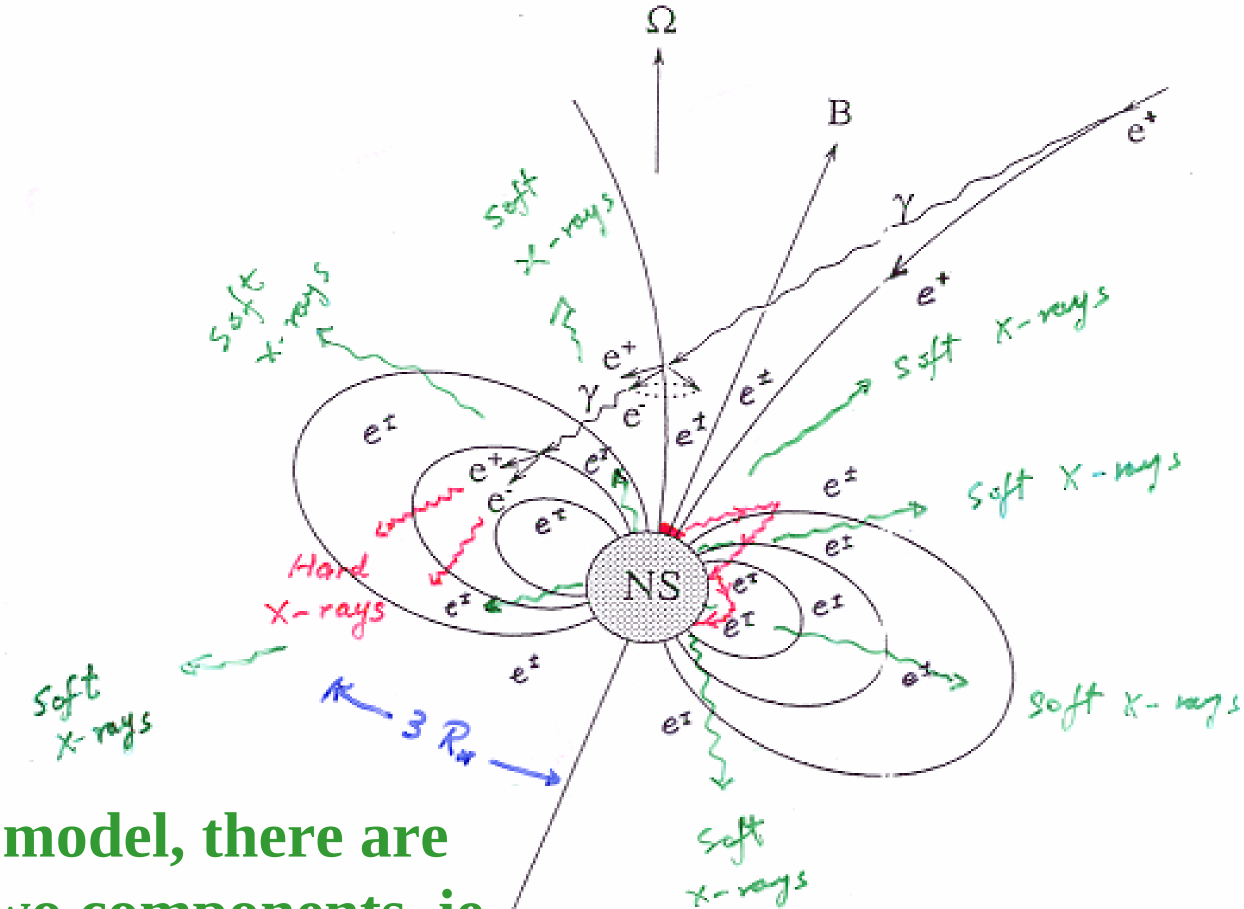

In this model, there are mainly two components, ie. BB from surface and PL from synchrotron radiation of cascade electron/positron

$$L_X = E_e(R)\dot{N}_e \approx 3.3 \times 10^{31} f B_{12} P^{-5/3}$$

$$L_X^n \approx 1.4 \times 10^{24} f^{-1/2} B_{12}^{5/4} P^{-17/4} \left(\frac{r_s}{R}\right)^2 x_{\min}^{-19/}$$

- In this model, the typical energies of the soft X-rays and the γ-rays are completely determined by pulsar parameters and the size of the outer gap
- Soft X-ray photon:

$$E_X \approx 9.8\times10^1 f^{1/4} B_{12}{}^{1/4} P^{-5/12}$$

- Curvature gamma-ray photon:

$$E_\gamma \approx 1.4\times10^8 f^{3/2} B_{12}{}^{3/4} P^{-7/4}$$

- Using pair production condition $E_X E_\gamma \sim (m_e c^2)^2$ we obtain:

$$\boxed{f \approx 5.5 B_{12}{}^{-4/7} P^{26/21}}$$

where $f \approx h/r_L$ is the fractional size of the gap

- **In this model we assume that if the gap current is weak the gap begins at the null charge surface, where the electric field is zero.**

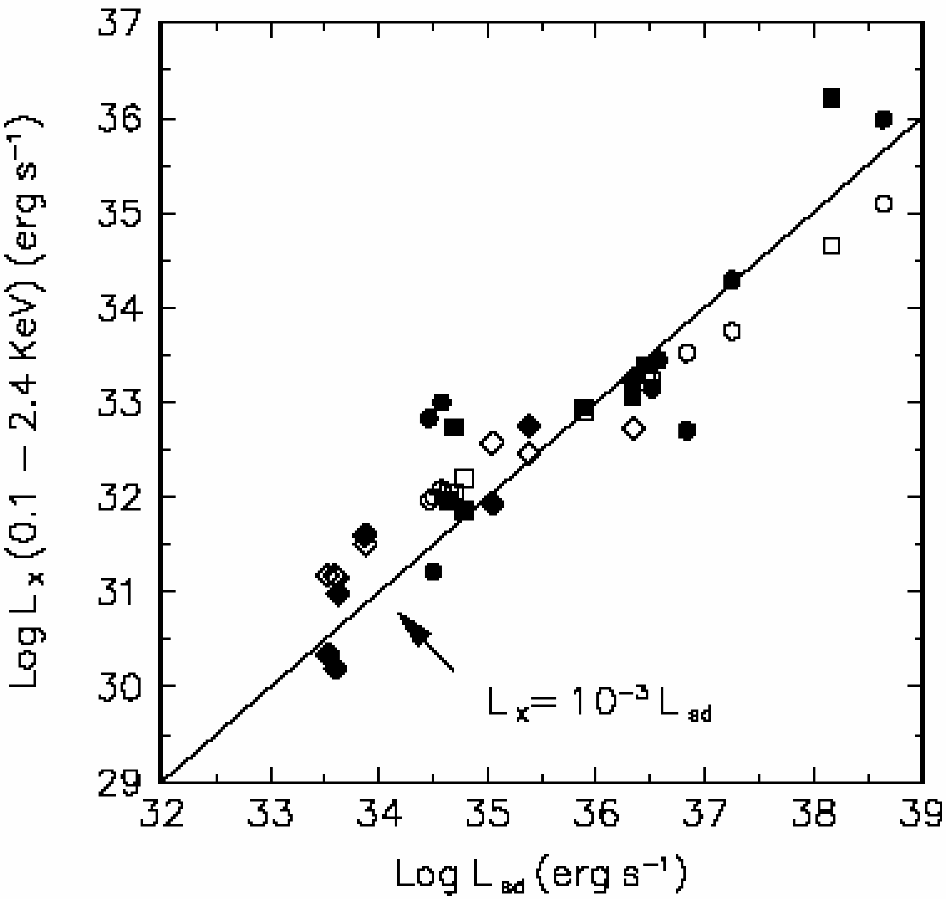

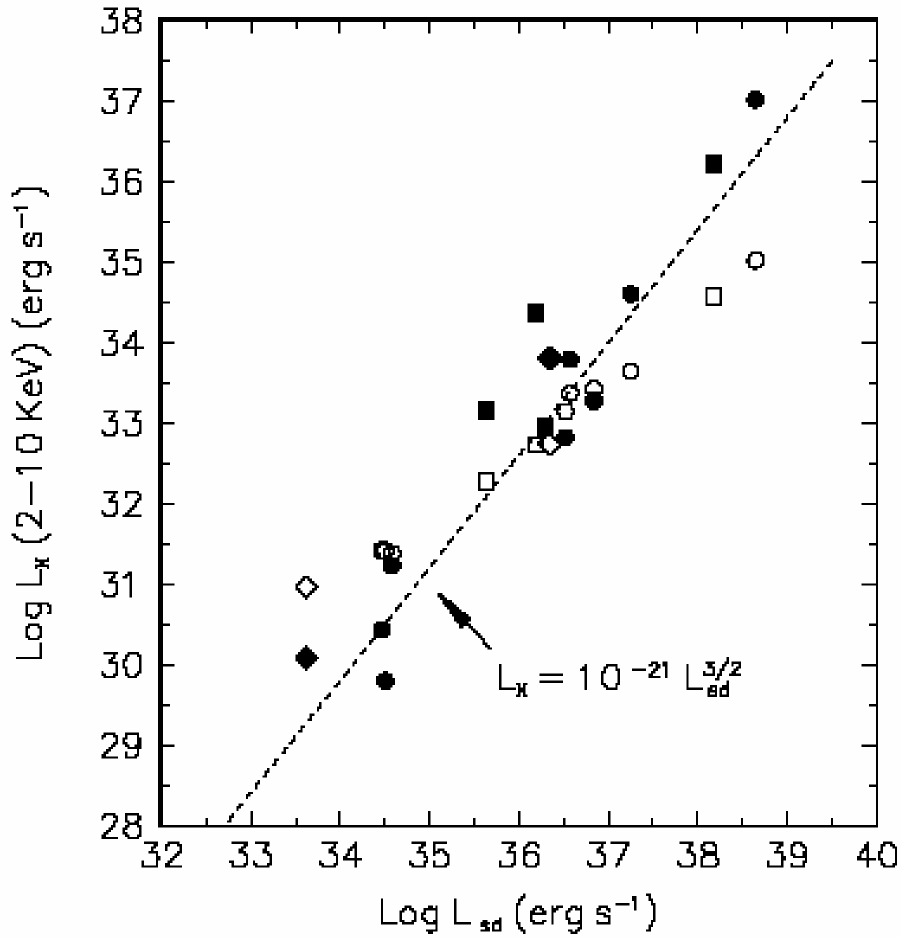

Solid symbols are data and empty symbols are model predictions

The model prediction (Cheng & Zhang 1999) in 2-10KeV is $L_x \sim (L_{sd})^{1.15}$, which is consistent with BT97 results in 0.1-2.4 KeV but inconsistent with the results of Saito et al. and Possenti et al.

Light curves

- The figure shows the photon emission direction. Once the observed angle is given, we can determine the light curve
- N.B. The emission direction is affected by the relativistic effects:
  - Aberration effect
  - Time of flight effect
- Consequently photon emission directions are squeezed into the boundary of the open field lines, a double peak structure is formed

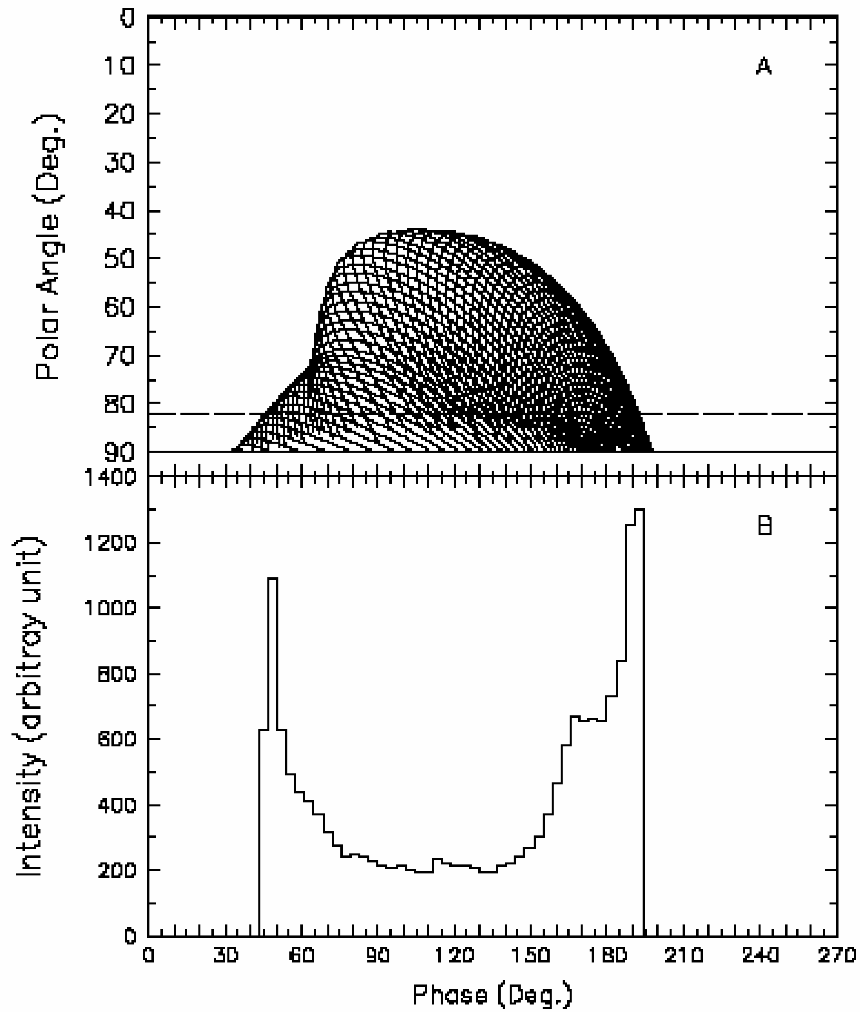

$\alpha = 65^{o}$ $\zeta = 81^{o}$

Calculation of Radiation Spectra -Trajectory of observed emission regions

Radial distance

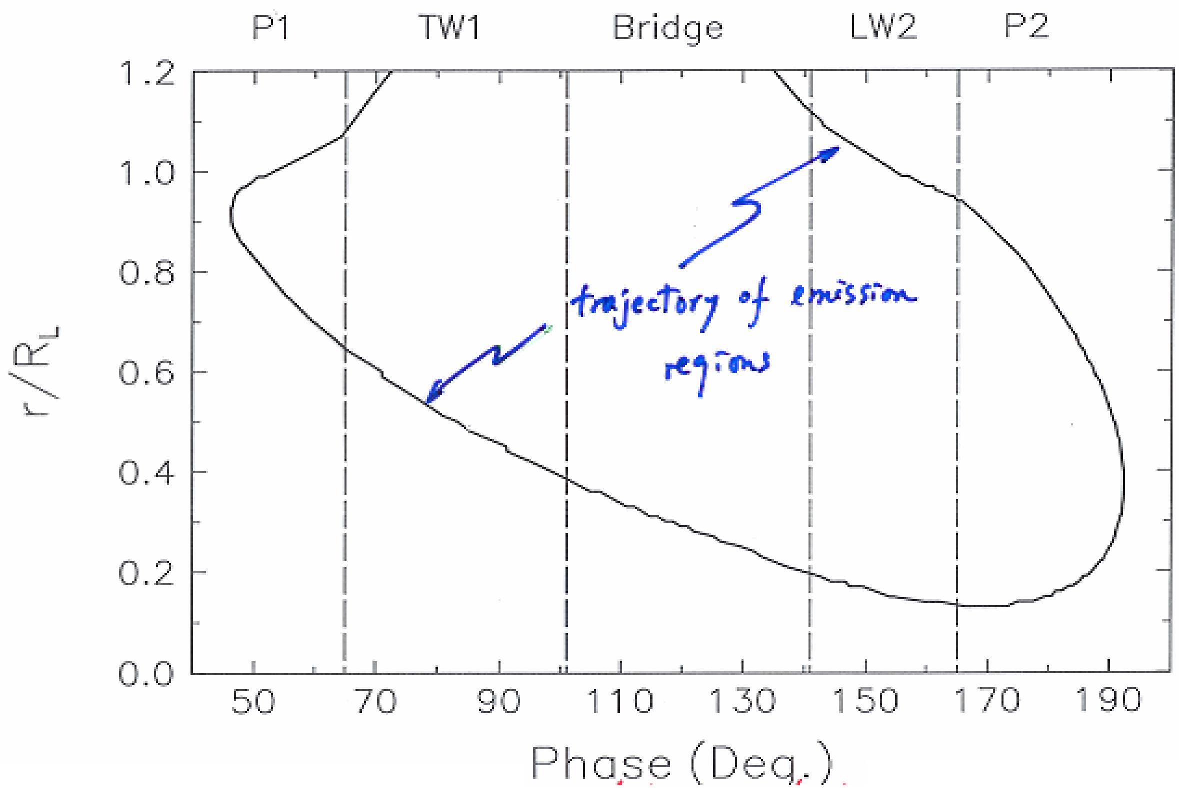

Calculate the local γ-ray emissivity including

curvature radiation,

synchrotron radiation and

inverse Compton scattering

EGRET Phase-resolved Spectrum of Crab Pulsar in Five Phases

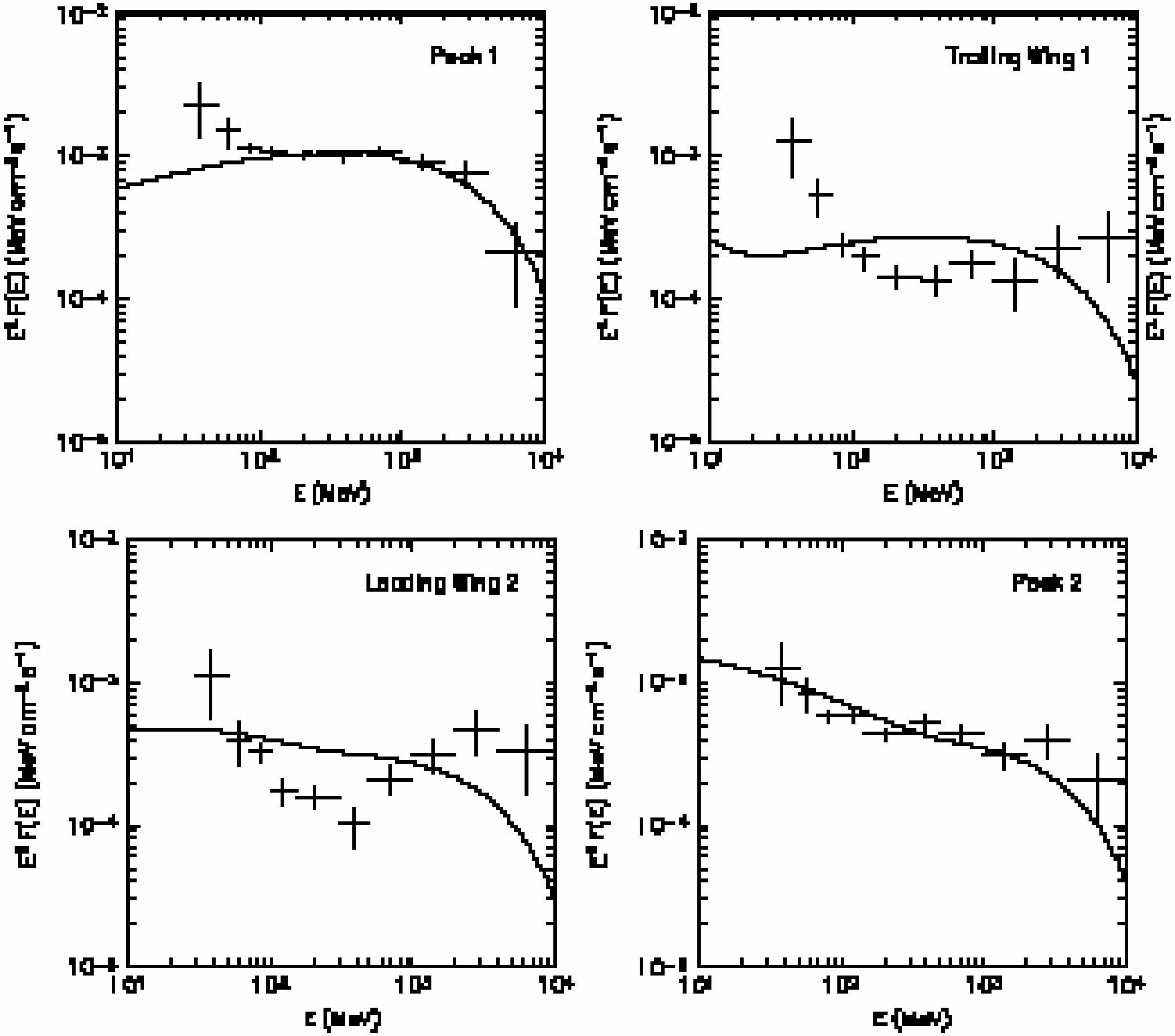

Because we have assumed the outer gap accelerator only exists from the null charge surface to the light cylinder. Consequently we can only produce radiation between two main peaks. Data outside this region cannot be explained in this geometry.

Problems of Geometry of CHR model

Maxwell eq: $\nabla \cdot E_{||} = 4\pi(\rho_e - \rho_{GJ})$

- Shibata, Hirotani, Takata et. al. (2003, 2004, 2005) they have pointed out that the assumed outer gap geometry will not be stable one when the electrodynamics is taken into account. The inner boundary of the outer gap will be no longer located at the null surface. The inner boundary will move toward the star when current flow is very large and near the Goldreich-Julian current density.

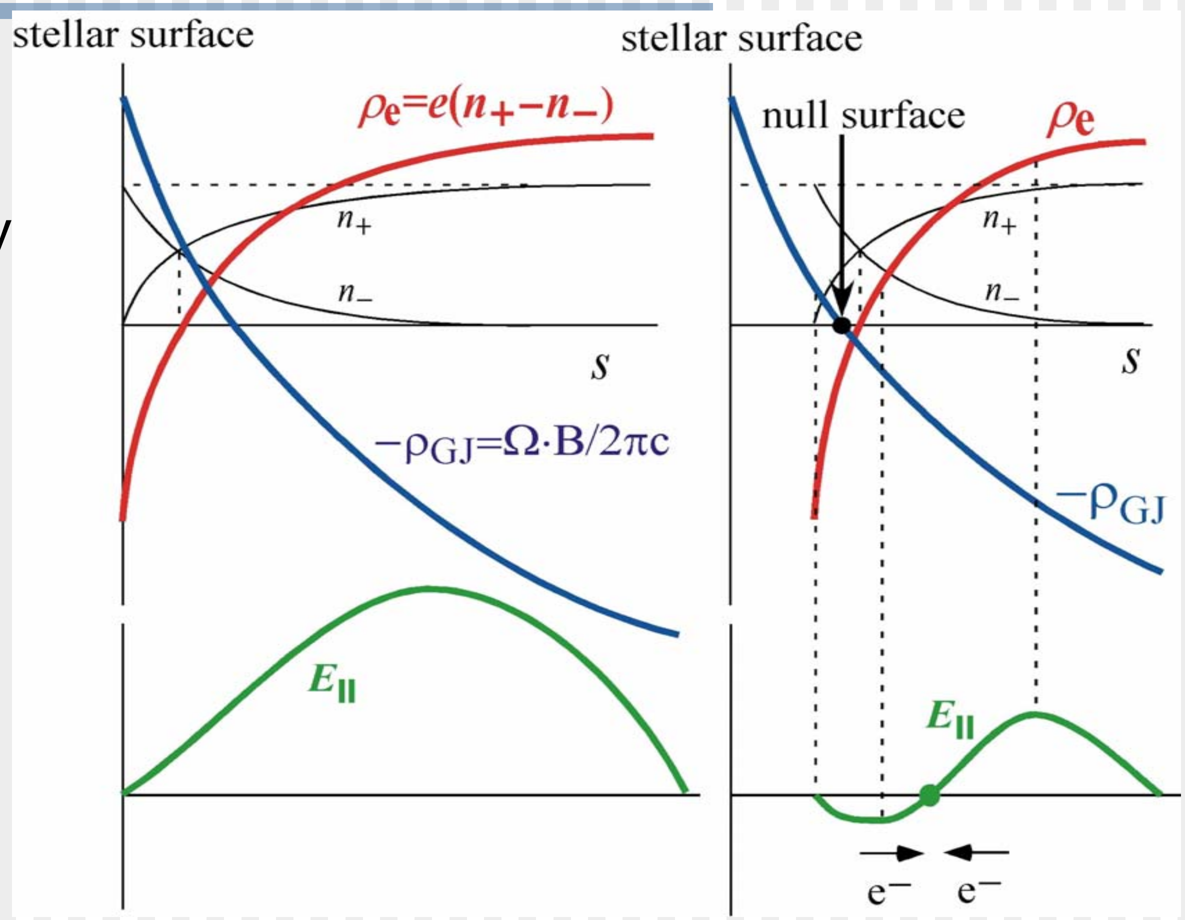

Hirotani 2005

Electric along B-field depends on the fraction of GJ current density (Hirotani 2005)

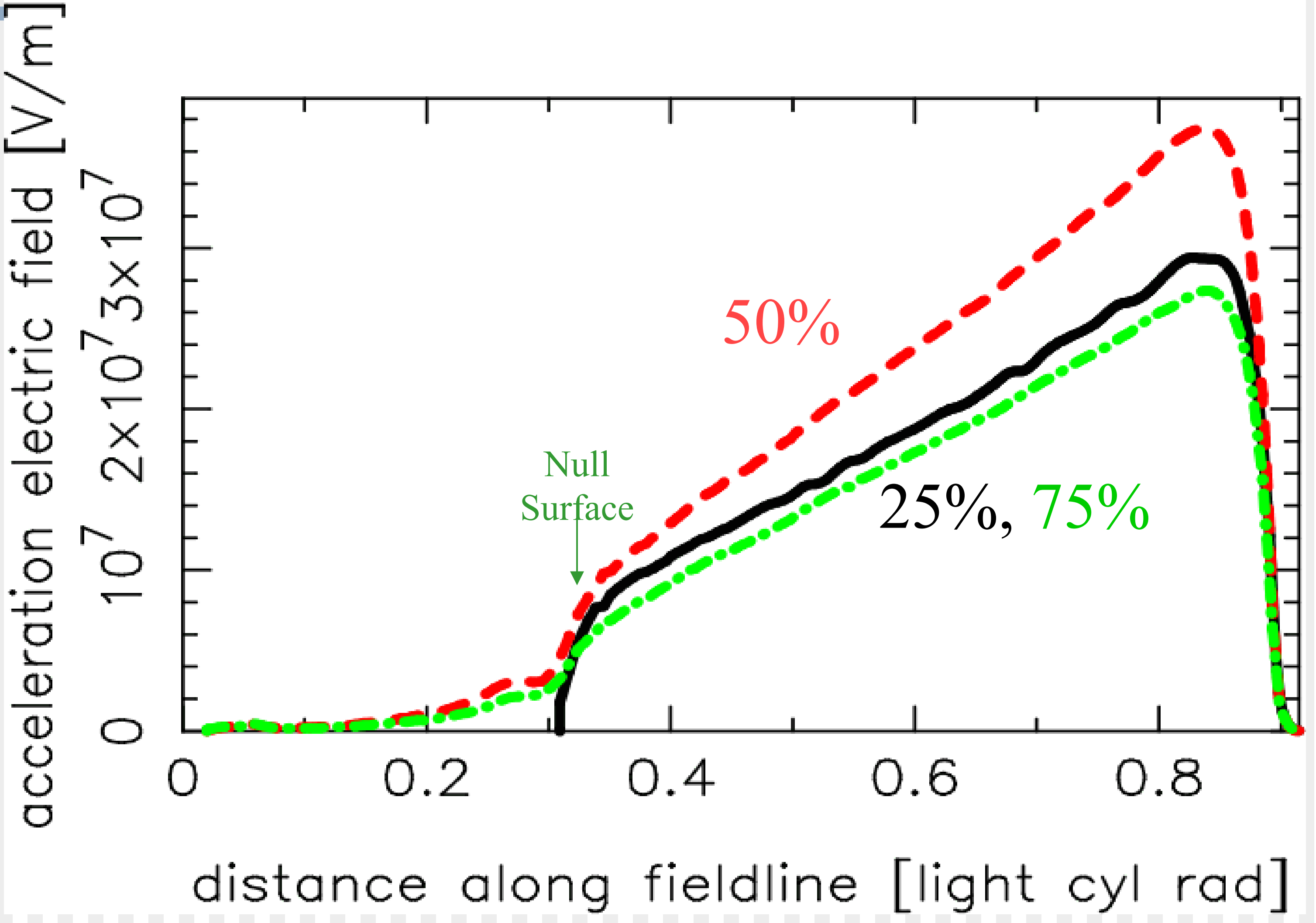

Light Curves and Emission Trajectories of New Geometry

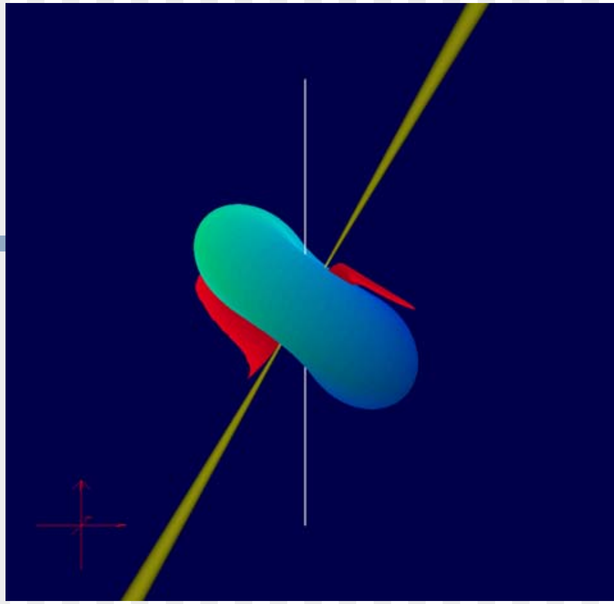

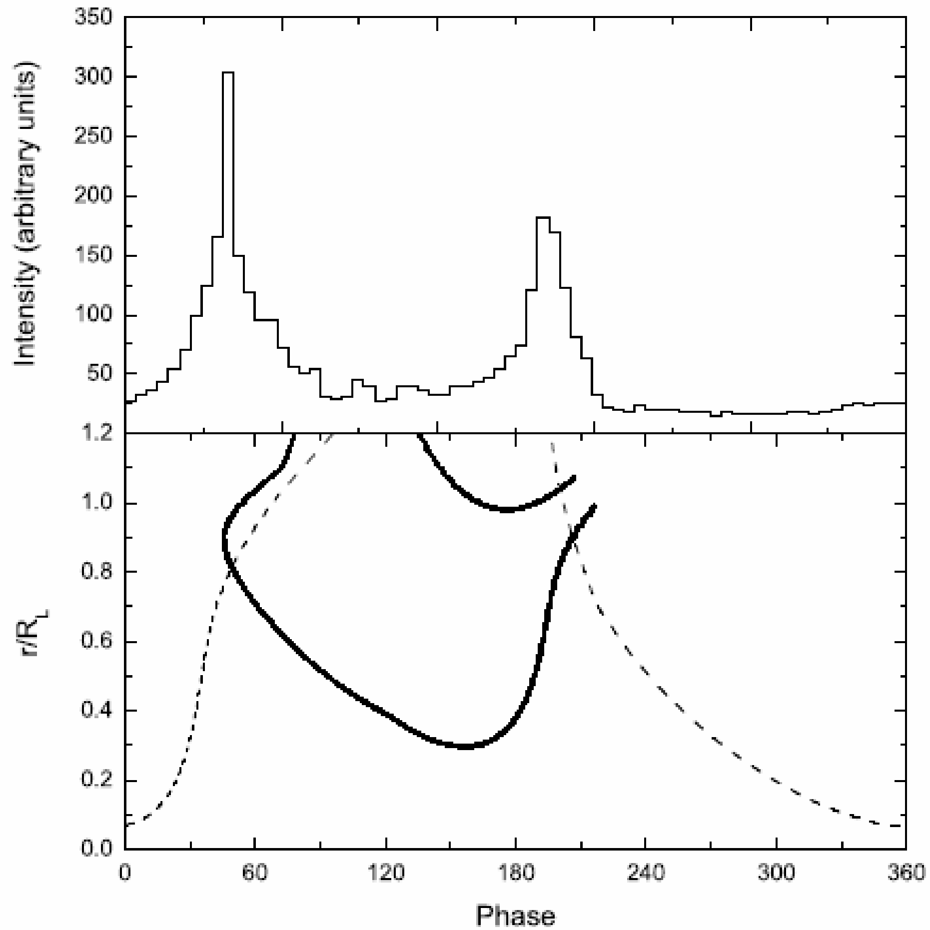

The solid curve is outgoing radiation of gap 1 from the null surface to the light cylinder and the dotted curve is the outgoing radiation of gap 2 from the inner boundary to the null surface.

In this new geometry of the accelerator, we can calculate the model phase resolved spectra to 360^0

Two parameters (B and Pitch angle) fitting of the phase-resolved spectra from 10^2 eV to 10^{10}eV for observed phases of the Crab pulsar ($\alpha=55^0$ and $\zeta= 80^0$) (Jia 2005)

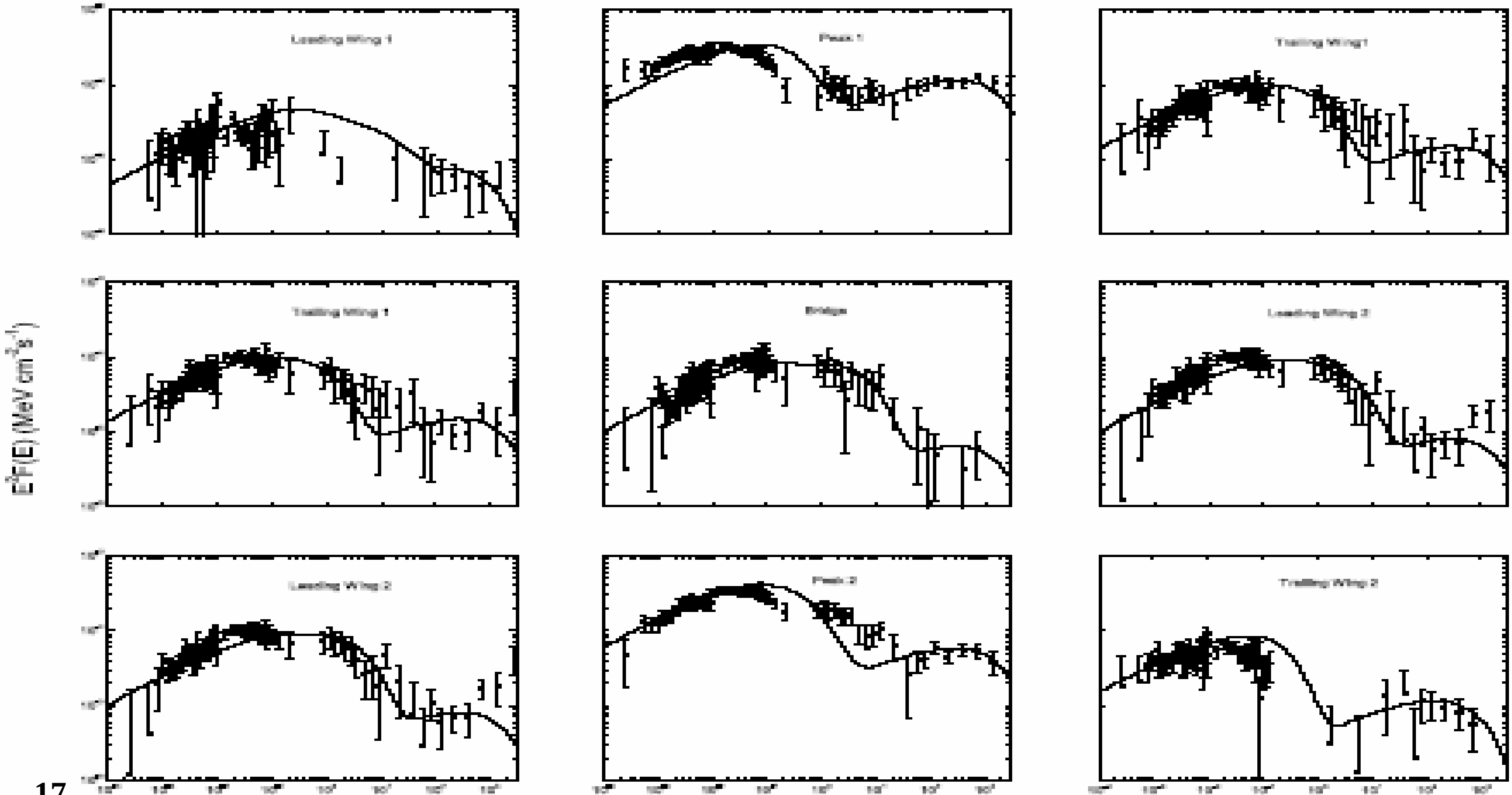

One parameter fitting (pitch angle) (Tang 2006)

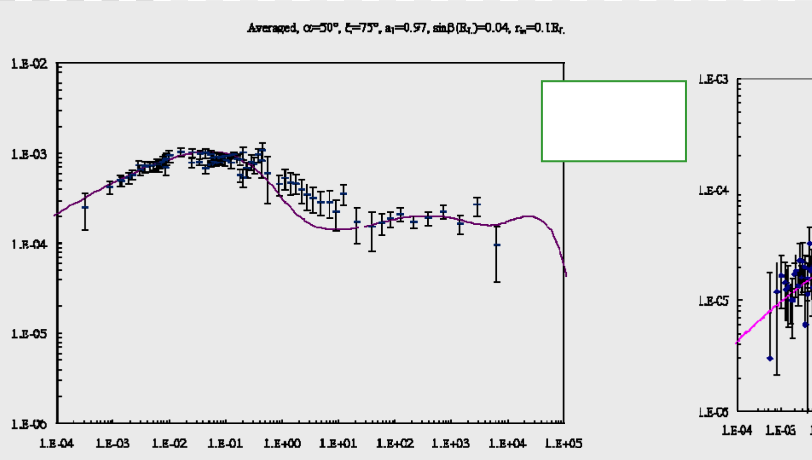

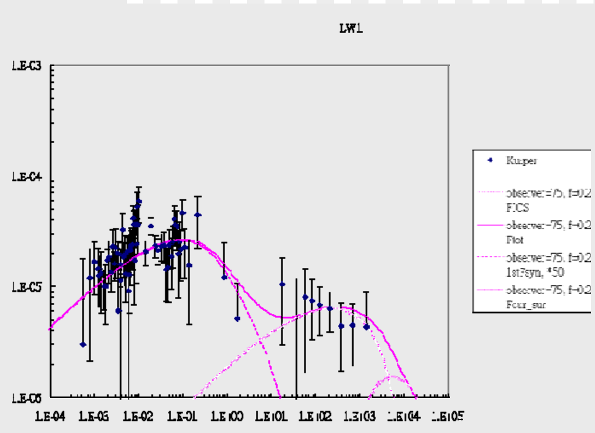

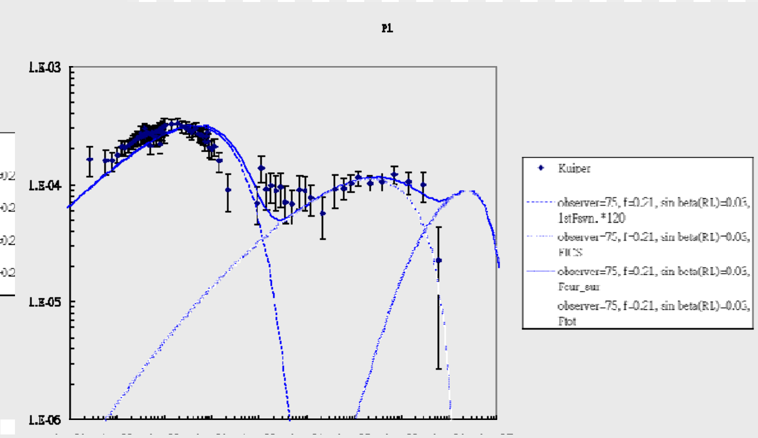

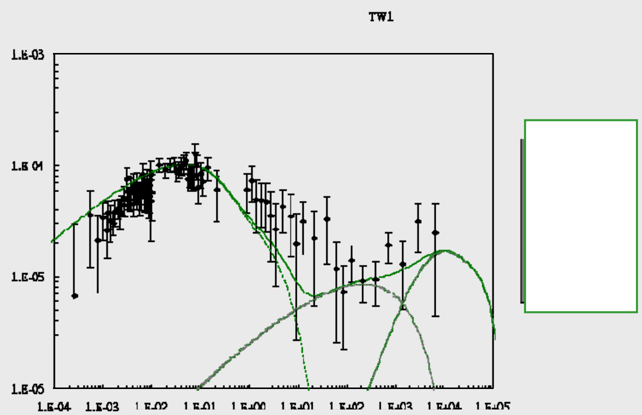

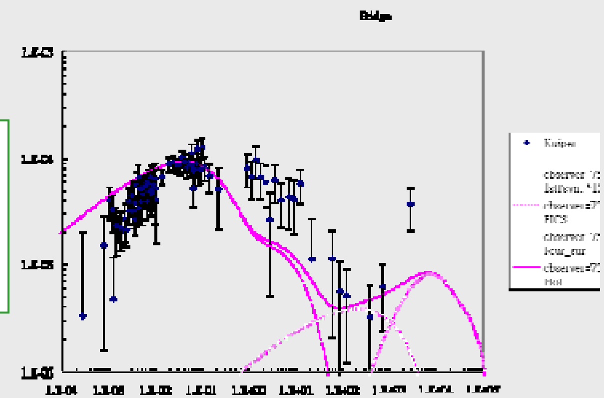

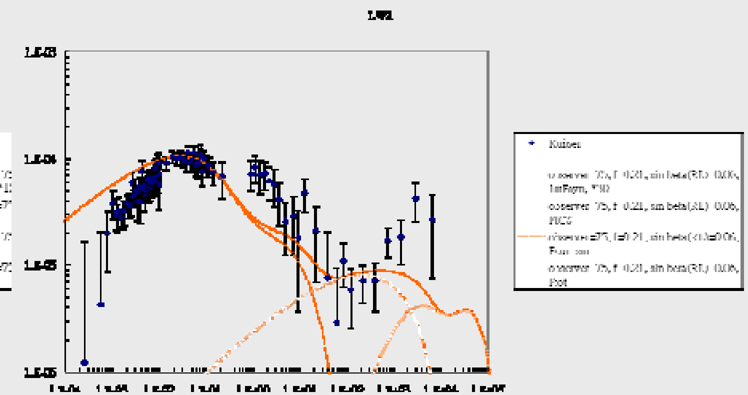

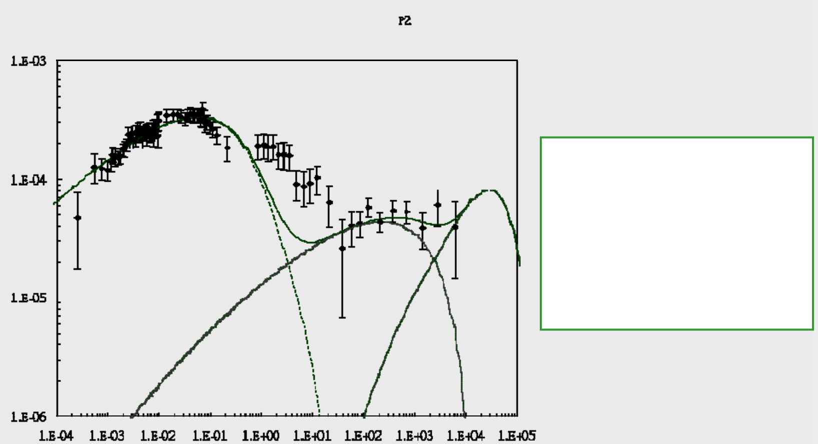

18

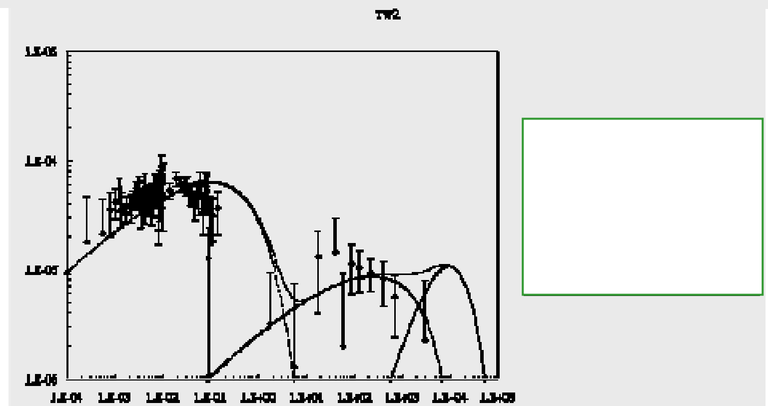

Detail calculation can be found in the poster in this conf. by J. Takata

Polarization of the Crab pulsar

- The optical data for the Crab pulsar has been available

1, K. Chen et al (1996)

-Polarization at two peaks with synchrotron emission

2, J.Dyks et al. (2004)

-Curvature emission model, which predicted too high degree of polarization

3, J.Petri & J.Kirk (2005)

-Pulsar strip wind model

Crab optical data

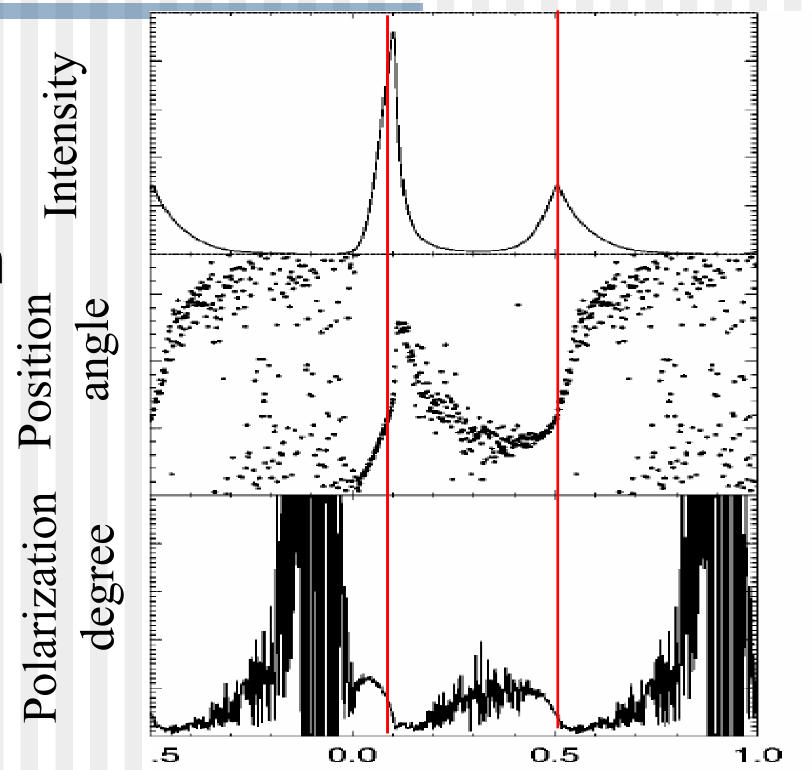

Kanbach et al 2004

They did not explain the Crab optical polarization data, optical spectrum and light curve together

J. Takata (2006)

Light curve

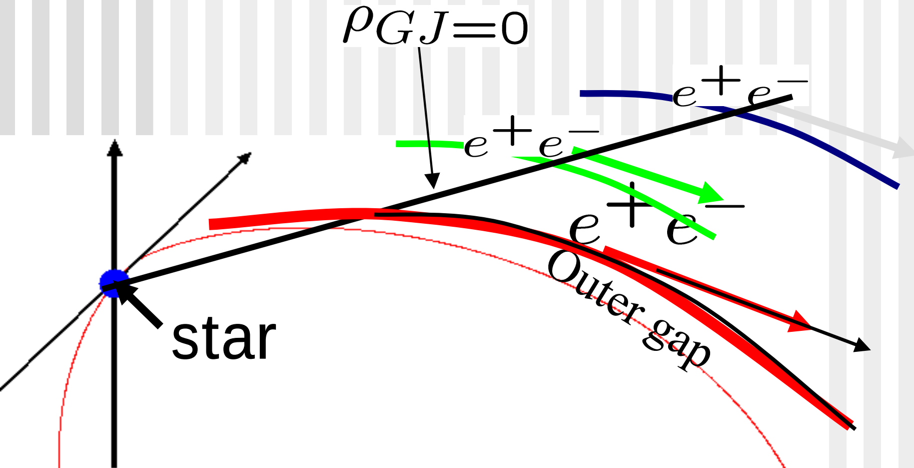

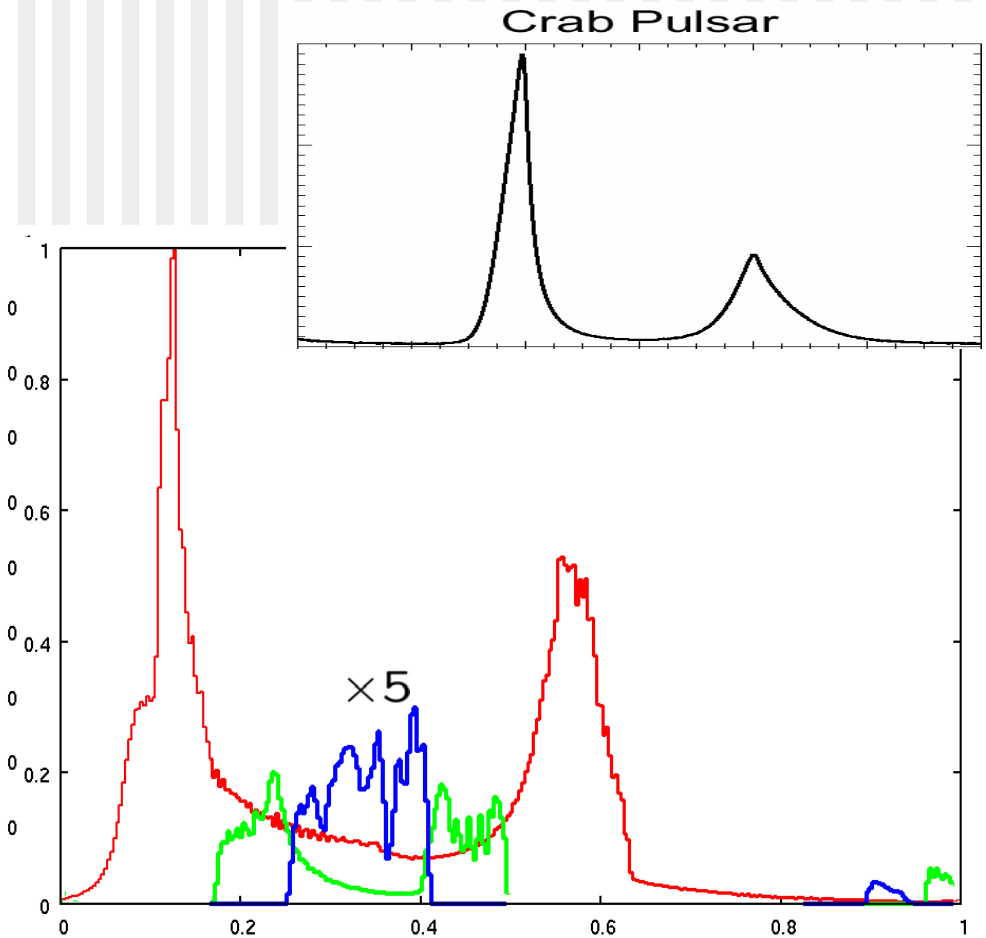

1. Outer gap starts from the inside of null charge surface
2. Emissions from higher order generated pairs

(<10% of peak flux of secondary pair emissions)

Optical polarization by traditional geometry

J. Takata (2006)

No off pulse

Low polarization between two peaks

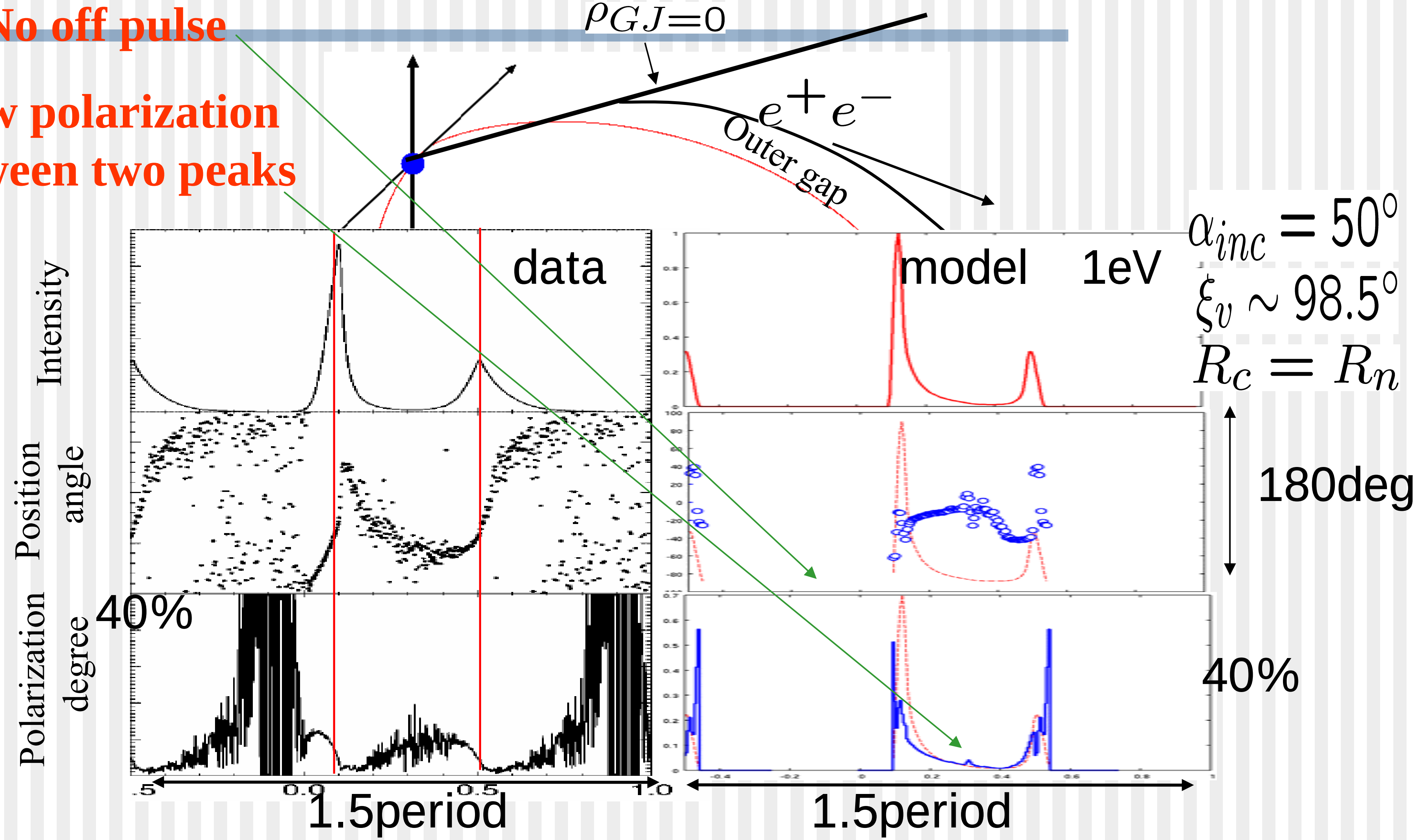

$\alpha_{inc} = 50^\circ$

$\xi_v \sim 98.5^\circ$

$R_c = R_n$

Modified outer gap model J. Takata (2006)

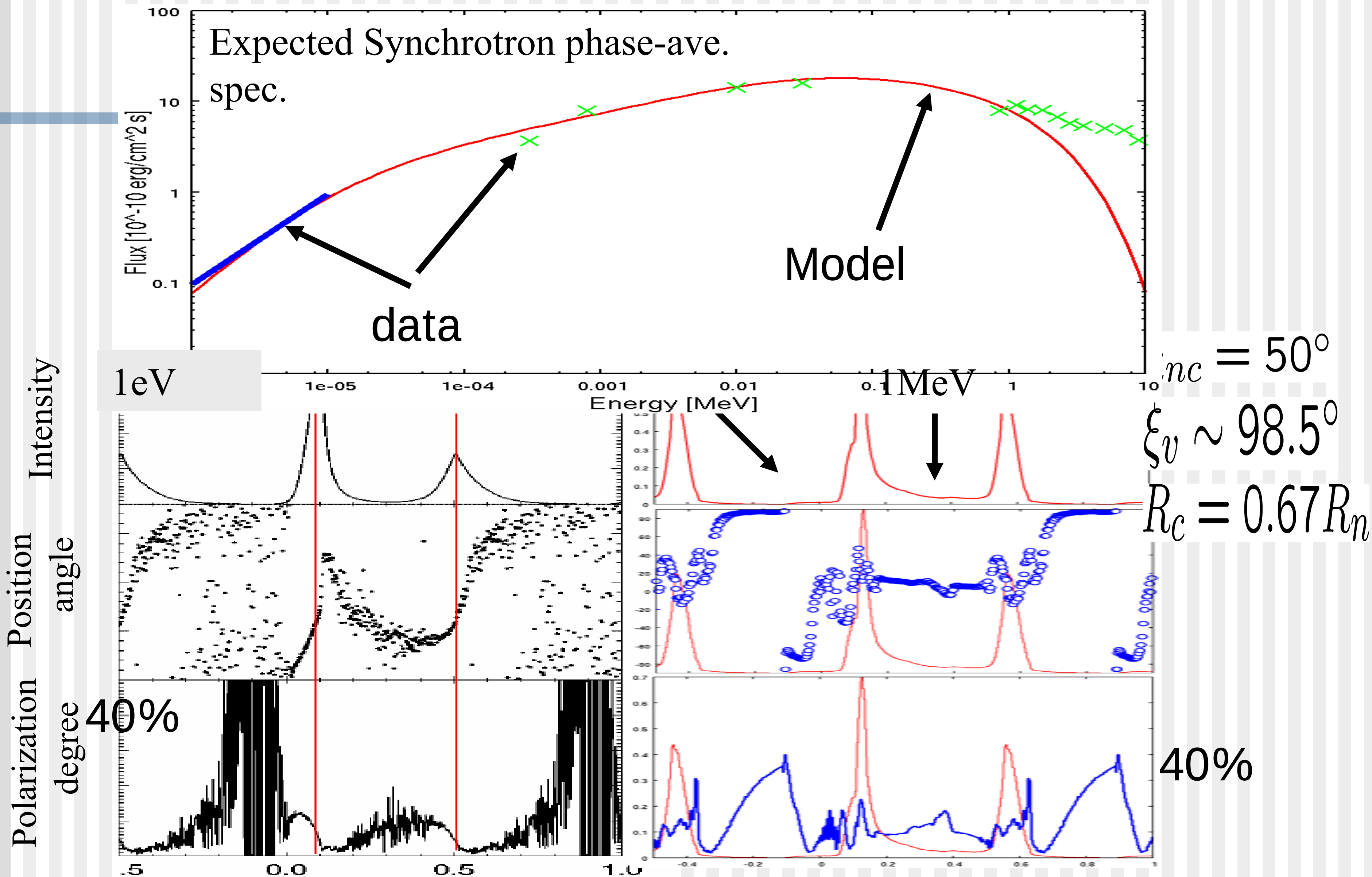

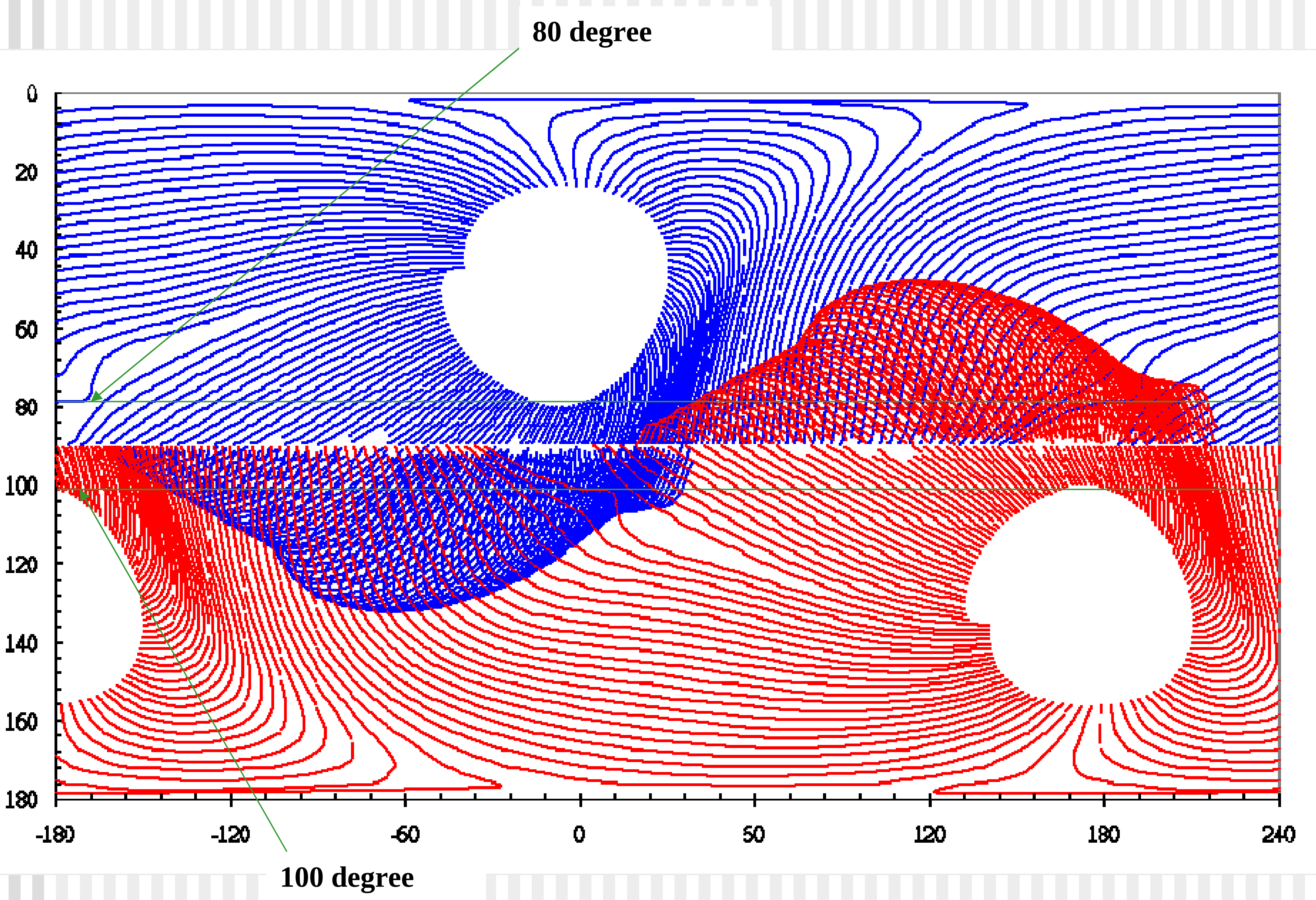

80 degree
0
20
40
60
80
100
120
140
160
180
-180
-120
-60
0
50
120
180
240
100 degree

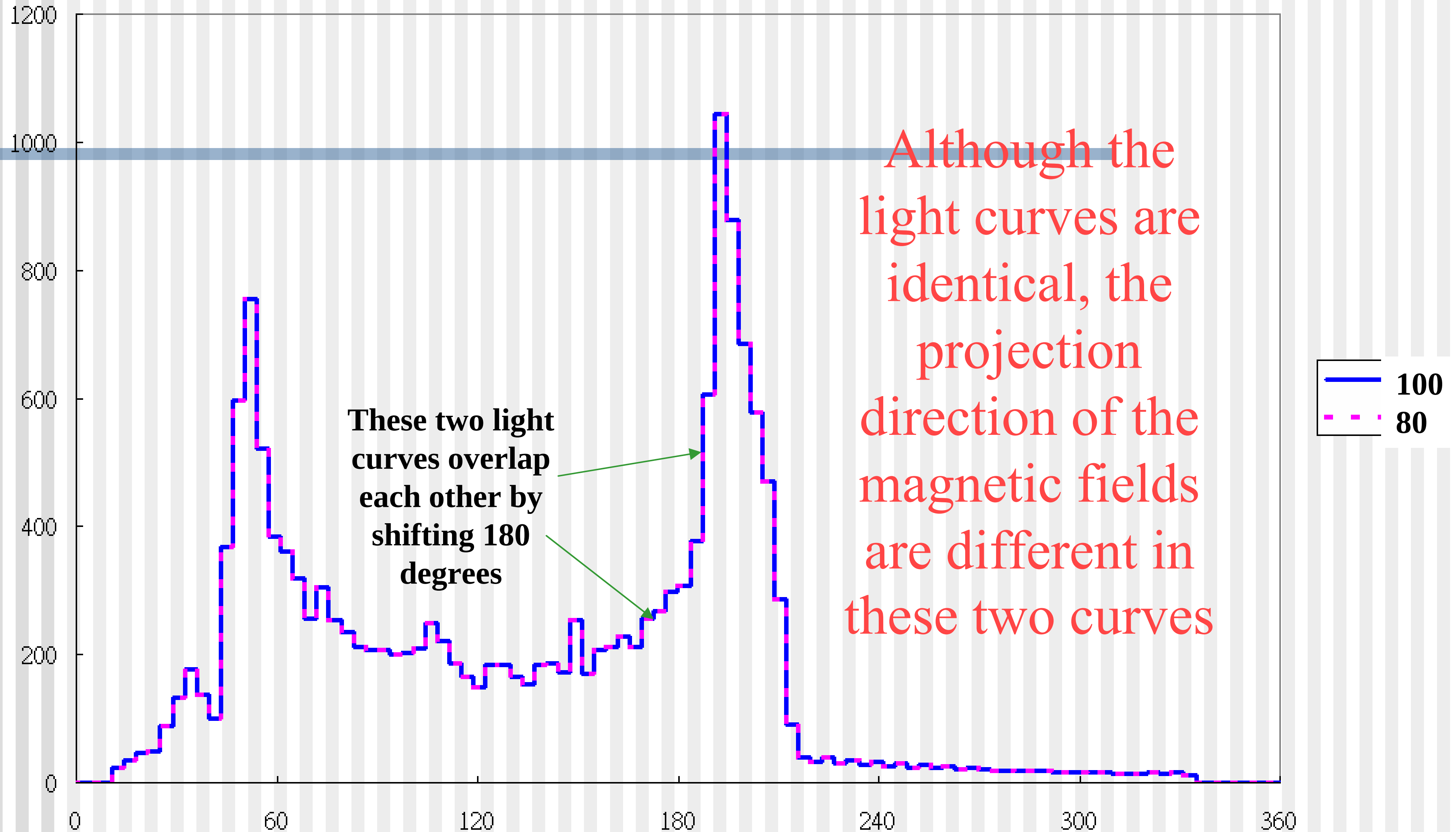
1200
1000
800
600
400
200
0
0
60
120
180
240
300
360
100
80
These two light curves overlap each other by shifting 180 degrees
Although the light curves are identical, the projection direction of the magnetic fields are different in these two curves

Viewing angle

J. Takata (2006)

- With position angle swing, we can determine the viewing angle from the rotation axis, which is ambiguous with light curves and spectrum.

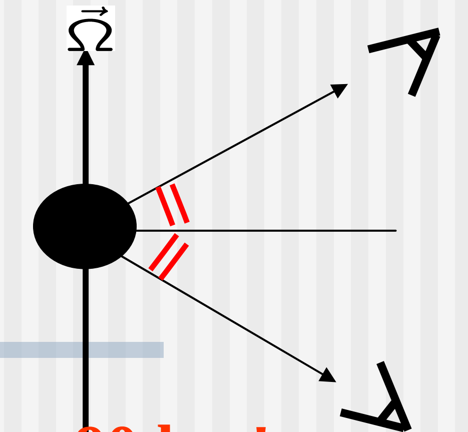

For the Crab pulsar, the viewing angle is lager than 90deg !

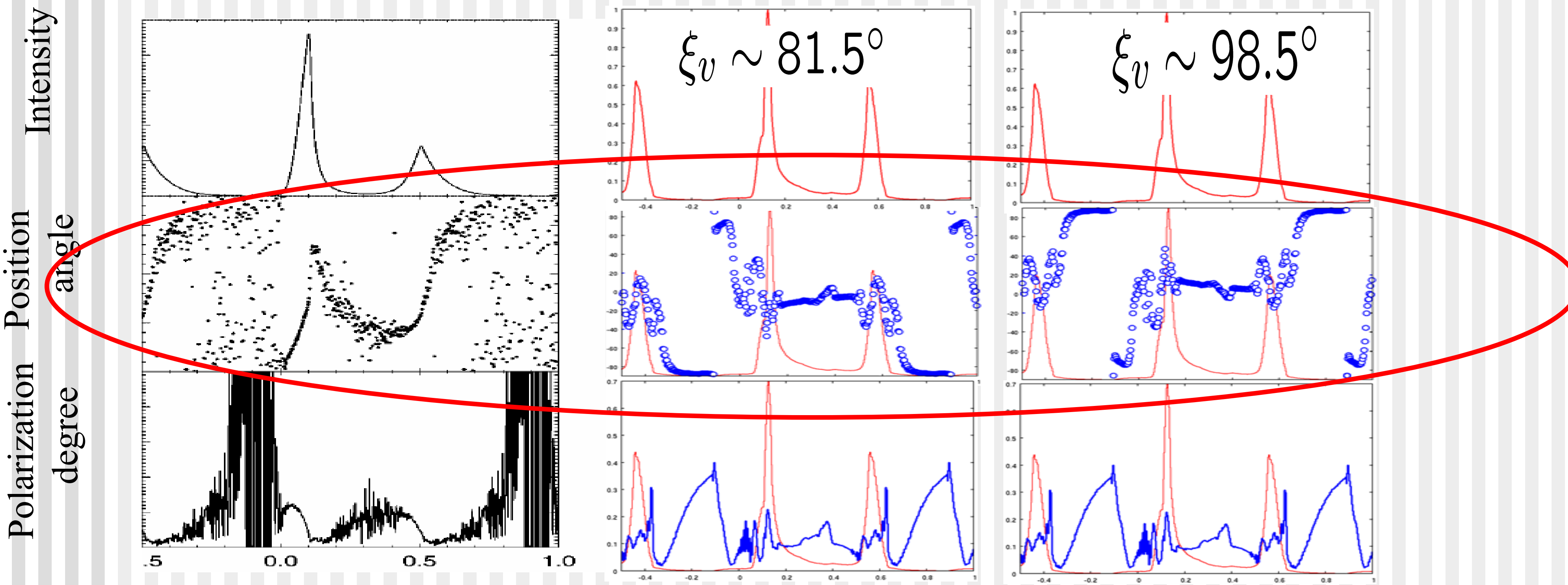

Radiation from PWN

- Shock will be formed when pulsar wind interacts with its surrounding SN/ISM and the shock radius is estimated as (for young pulsars)

$$R_s \simeq (\frac{L_{\rm sd}}{B^2 c})^{1/2} \sim 6\times 10^{14} L_{\rm sd,34}^{1/2} B_{mG}^{-1}{\rm cm}$$

(For mature and millisecond pulsars)

$$R_s \simeq (\frac{L_{\rm sd}}{2\pi\rho_{\rm ISM} v_p^2 c})^{1/2} \sim 3\times 10^{16} L_{\rm sd,34}^{1/2} n_1^{-1/2} v_{\rm p,100}^{-1}{\rm cm},$$

- Synchrotron radiation from the relativistic electrons gives non thermal X-ray with (Chevalier 2000)

$$L_x \propto \epsilon_e^{p-1} \epsilon_B^{(p-2)/4} \gamma_w^{p-2} R_s^{-(p-2)/2} L_{\rm sd}^{(p+2)/4}$$

Where 2<p<3 is the electron power index.

Recently we re-examine ASCA data and find $L_x \sim (L_{sd})^{1.35}$ similar to that of Possenti et al. (Cheng, Taam & Wang 2004). HOWEVER

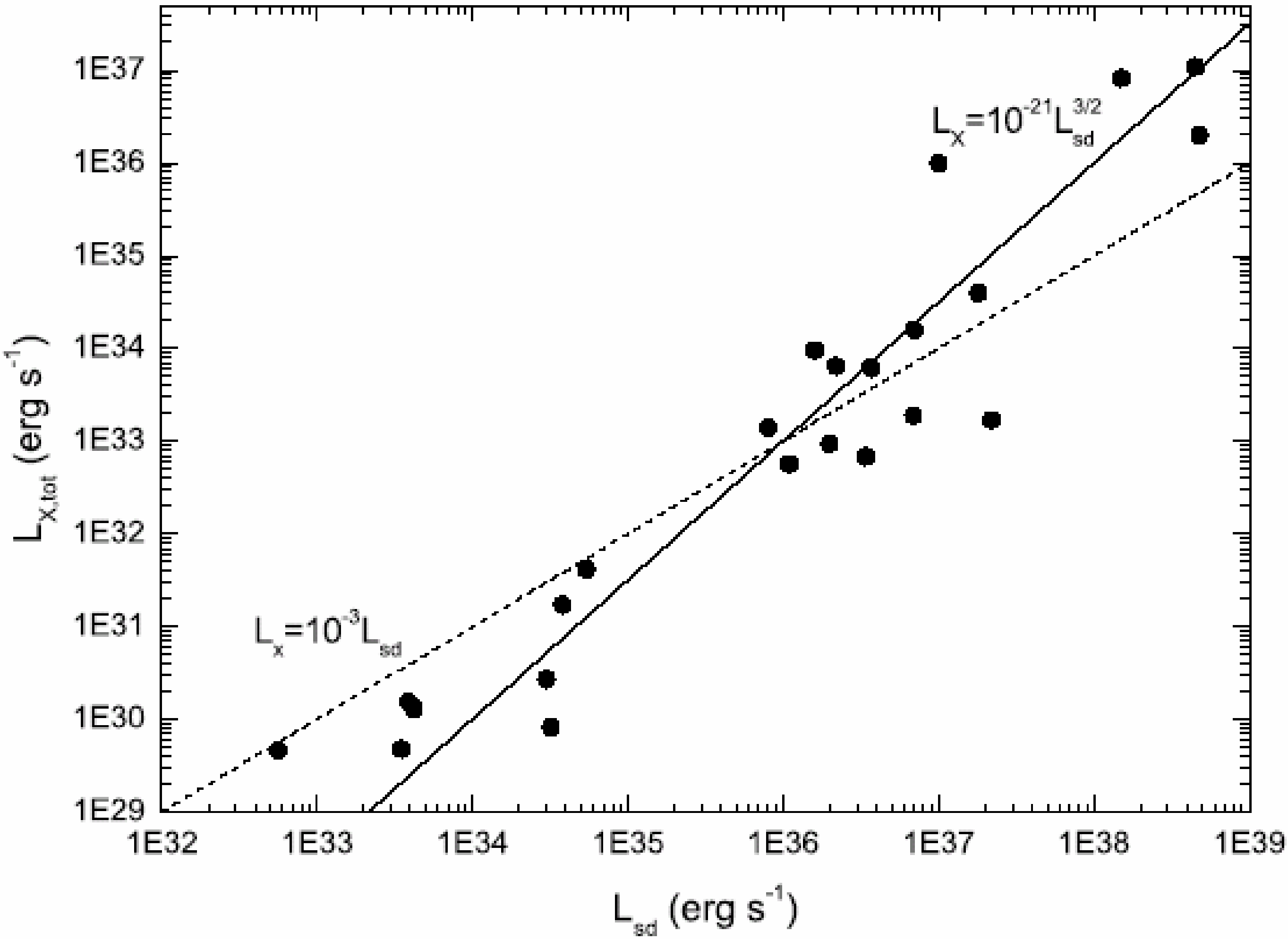

References: 1. Torii et al. 2001; 2. Torii et al. 1997; 3. Torii et al. 1999; 4. Saito et al. 1997a; 5. Helfand, Gotthelf & Halpern 2001; 6. Pavlov et al. 2001; 7. Halpern & Wang 1997; 8. Cavaveo et al. 2003; 9. Pivovaroff et al. 2000; 10. Wang & Halpern 1997; 11. Hirayama et al. 2002; 12. Shibata et al. 1997; 13. Halpern et al. 2001; 14. Marshall et al. 1998; 15. Wang & Gotthelf 1998; 16. Gotthelf et al. 2000; 17. Takahashi et al. 2001; 18. Sakurai et al. 2001; 19. Saito et al. 1997b.

Separating pulsed and non pulsed components in ACSA data

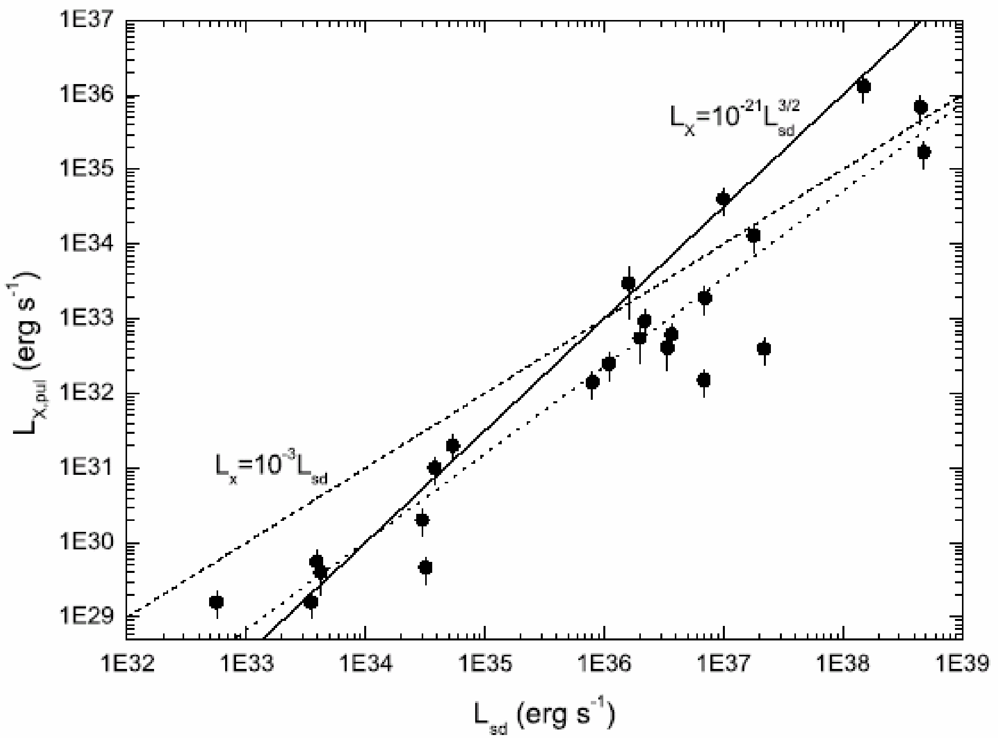

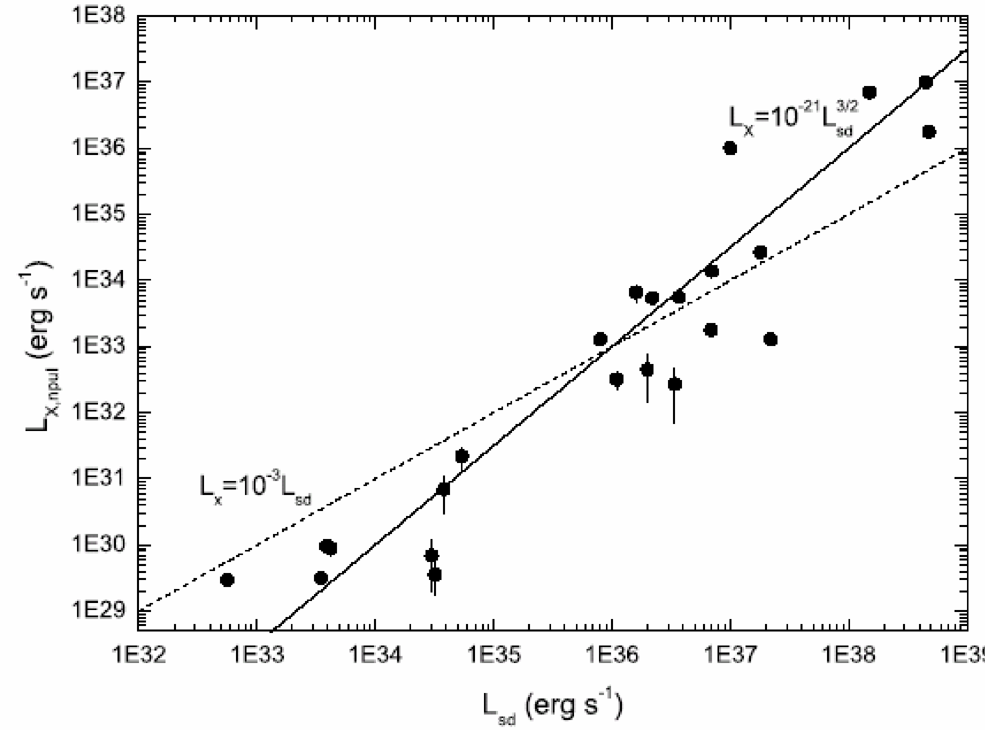

$(L_x)^{pul} \sim (L_{sd})^{1.15}$

This is consistent with BT97 and our model prediction for X-rays from magnetosphere

$(L_x)^{np} \sim (L_{sd})^{1.4}$

This component must come from outside the magnetosphere, e.g. PWN

Relation between L_x and L_{sd} of PWN

$$L_x \propto \epsilon_e^{p-1} \epsilon_B^{(p-2)/4} \gamma_w^{p-2} R_s^{-(p-2)/2} L_{sd}^{(p+2)/4}$$

Assume proton/ion flux in PW is GJ flux

$$\dot{N} \simeq 1.35 \times 10^{30} B_{12} P^{-2} \mathrm{s}^{-1}$$

Since $L_{sd} \simeq 10^{31} B_{12}^2 P^{-4} \mathrm{erg\ s}^{-1}$, we find $\dot{N} \propto L_{sd}^{1/2}$, leading to $\gamma_w \propto L_{sd}^{1/2}$. recall $R_s \propto L_{sd}^{1/2}$

These together give $L_X \propto L_{sd}^{p/2}$;

It appears that the observed relation between should be ~1.25 instead of 1.34 (Possenti et al. 2002) if the distribution of p is uniform. However, observations tend to pick up more luminous sources which may bias to large “p”.

Assuming $\varepsilon_e \sim 0.5$, $\varepsilon_B \sim 0.01$ and $p = 2.2$, we obtain

PSR	L_{sd}	R_s^{obs} cm	R_s^{th} cm	L_{upul}^{obs}	L_{upul}^{th}	n cm^{-3}	v_p km s^{-1}
B1823-13	2.8×10^{36}	6×10^{17}		3×10^{33}	3×10^{33}	1	
J0537-6910	4.8×10^{38}	4×10^{17}		1.8×10^{36}	4×10^{36}		
B0540-69	1.5×10^{38}	3×10^{17}		7×10^{36}	5×10^{36}		
J1811-1926	7×10^{36}	2×10^{17}		1.4×10^{34}	10^{34}		
B0531+21	4.5×10^{38}	4×10^{17}	3×10^{17}	10^{37}	5×10^{36}	10	123
B0833-45	6.9×10^{36}	10^{17}	2×10^{17}	1.8×10^{33}	10^{33}	1	65
B0633+17	3.2×10^{34}	5×10^{16}	4×10^{16}	4×10^{29}	10^{30}	1	120
J2229+6114	2.2×10^{37}	4×10^{17}		1.3×10^{33}	2×10^{33}		
J1105-6107	2.5×10^{36}	4×10^{16}		4×10^{33}	3×10^{33}		
B1706-44	3.4×10^{36}	3×10^{17}		3×10^{32}	3×10^{32}		
B1757-24	2.6×10^{36}	4×10^{16}	$> 5\times10^{16}$	3×10^{32}	4×10^{32}	1	< 590
J0205+6449	2.6×10^{37}	10^{17}		3×10^{34}	3×10^{34}		
B1957+20	10^{35}	5×10^{16}	4×10^{16}	10^{31}	2×10^{31}	1	220
J2021+3651	3.6×10^{36}	8×10^{17}		3×10^{33}	10^{33}		
J1747-2958	2.5×10^{36}	3×10^{16}	7×10^{16}	5×10^{34}	10^{34}	0.3	600
J1124-5916	10^{37}	10^{17}	2×10^{17}	4×10^{34}	10^{34}	0.5	450
B1853+01	4.3×10^{35}	10^{17}	3×10^{16}	6×10^{32}	4×10^{32}	5	375
J1930+1852	2×10^{36}	10^{17}		10^{33}	6×10^{32}	1	
B0453-685	10^{37}	6×10^{17}		6×10^{34}	10^{34}	0.4	
J0538+2817	4×10^{34}	8×10^{16}	3×10^{16}	6×10^{31}	5×10^{31}	0.5	385

Why does L_x of MSPs in the field and in the 47 Tuc obey different L_{sd} relation?

- Similarities – period, dipole magnetic field and orbital period.
- Observational hints :

(1)The observed mean Lx ~ 2 $x10^{30}$ erg/s but the observed spectrum is thermal with an almost constant T ~ $3x10^6$ K. These two quantities suggest that the polar cap radius is only ~$3x10^4$ cm, which is much smaller than the polar cap radius of dipolar field ~$3x10^5$ cm. This may suggest some strong but small scale field exists on the surface MSPs in 47 Tuc.

(2)This temperature is extremely insensitive to L_{sd}

(3) MSPs in 47 Tuc are not good gamma-ray emitters.

- Differences –

(1) the actual long age of MSPs(> billion yrs) in globular cluster may allow the **complex** field structure created during the accretion phase but bury deep inside the star diffuse out to the surface.

(2)Several times of exchanging companion also make the field lines complicated.

What are effects of complicated surface field?

(1)Strong multiple surface field can turn off the outer gap. In this case, X-rays only come from the polar cap heating and PWN

(2)strong multiple surface can greatly reduce the polar cap area

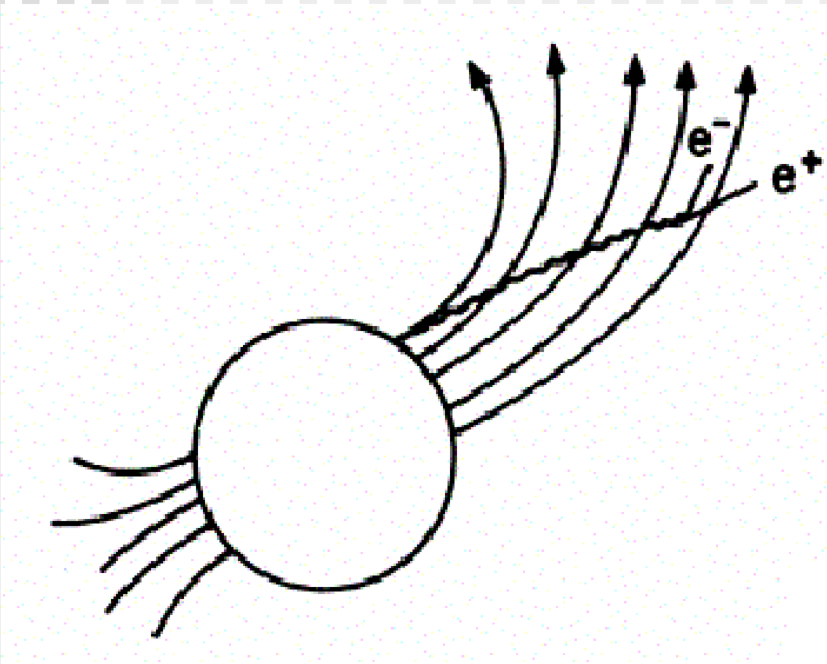

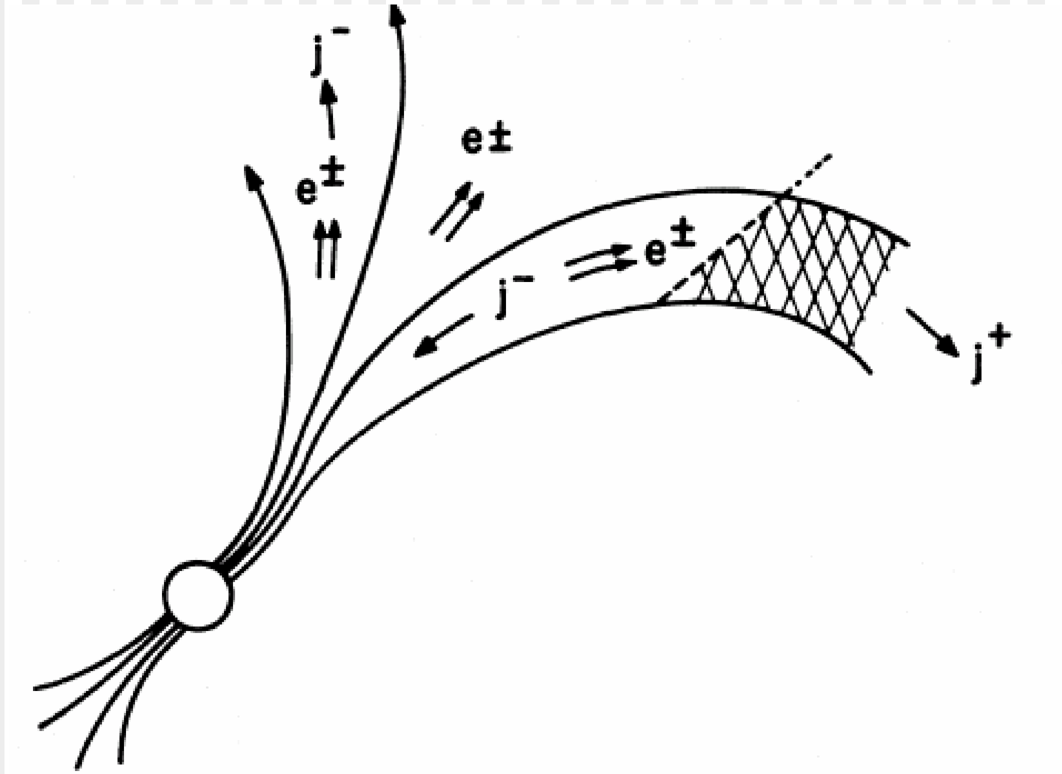

Ruderman and Cheng 1988

Thermal X-rays from polar cap

Polar cap heating is given by $\mathbf{L_x = J_{GJ}\, V_{gap}}$ where J_{GJ} is the Goldreich-Julian current and V_{gap} is the potential of the polar gap.

Since

$$J_{GJ} = 1.35 \times 10^{30} B_{12} P^{-2}\ e\ s^{-1}$$

and

$$L_{sd} = 3.8 \times 10^{31} B_{12}^{2} P^{-4}\ \mathrm{ergs\ s^{-1}}$$

We can see that if V_{gap} is constant or insensitive to *B* and *P* then $L_x \sim (L_{sd})^{1/2}$. There are three known models which are satisfied this requirement, e.g. RS75 :

$$V_{RS} = 10^{12} B_{12}^{-1/7} P^{-1/7} s_6^{4/7}\ \mathrm{V}$$

which implicitly require small scale and strong surface magnetic field (>> the observed dipole field of MSPs)

Why MSPs in 47 Tuc do not have non thermal contribution from PWN?

millisecond pulsars and their X-ray properties

	D (kpc)	n (cm^{-3})	$v_p^{\dagger}$ ($km\ s^{-1}$)	$\delta\theta$	R_{obs} (cm)	R_s (cm)	L_X
1957+20	1.5	1	220	5”	6×10^{16}	5×10^{16}	nonthermal
47 Tuc	5	0.1	60	1”	3.5×10^{16}	2×10^{17}	thermal

Therefore MSPs in 47 Tuc only have THERMAL X-rays from polar cap heating and no contribution from outer gap (non thermal).

Consequently L_x $(L_{sd})^{1/2}$

Conclusions

- X-rays from MSPs with small scale strong multipole surface magnetic field should be thermal and $L_X \alpha (L_{sd})^{0.5}$. Outer gap should not exist in these pulsars and hence they should be weak gamma-ray emitters.
- Pulsars with outer gap should have the pulsed X-ray component coming from the pulsar magnetosphere with $L_X \alpha (L_{sd})^{1.15}$
- The non-pulsed non thermal component of X-ray pulsars should come from the PWN with $L_X \alpha (L_{sd})^{p/2}$
- Polarization, light curves and phase-resolved spectra must be explained by 3D pulsar model
- The phase-resolved spectrum of the Crab pulsar consists of three components, i.e. synchrotron radiation, ICS and curvature radiation
- The break in ultra-violet results from small pitch angle in synchrotron radiation and most important the swing of polarization angle suggests that the viewing angle must be larger than 90 degree.